Structure of the micronemal protein 2 A/I domain from Toxoplasma gondii

ARTICLE *in* PROTEIN SCIENCE · OCTOBER 2010

Impact Factor: 2.85 · DOI: 10.1002/pro.477 · Source: PubMed

5 AUTHORS, INCLUDING:

Michelle L Parker
University of Victoria
26 PUBLICATIONS **273** CITATIONS
SEE PROFILE

Mark Pearce
University of British Columbia - Vancouver
5 PUBLICATIONS **60** CITATIONS
SEE PROFILE

PROTEIN STRUCTURE REPORT

Structure of the micronemal protein 2 A/I domain from *Toxoplasma gondii*

Michelle L. Tonkin, Ognjen Grujic, Mark Pearce, Joanna Crawford, and Martin J. Boulanger*

Department of Biochemistry and Microbiology, University of Victoria, Victoria, British Columbia V8W 3P6, Canada

Received 4 June 2010; Accepted 21 July 2010
DOI: 10.1002/pro.477
Published online 3 August 2010 proteinscience.org

Abstract: *Toxoplasma gondii* is a widespread zoonotic pathogen capable of causing serious disease in humans and animals. As an obligate intracellular parasite, *T. gondii* relies on the orchestrated secretion of proteins from its apical complex organelles including the multimodular, transmembrane micronemal protein 2 (MIC2) that couples recognition of the host cell with cytoskeletal reorganization of the parasite to drive invasion. To probe the basis by which the von Willebrand Factor A (vWA)–Integrin like module of TgMIC2 engages the host cell, we solved the crystal structure of a truncated form of TgMIC2A/I (TgMIC2A/Ic) phased by iodide SIRAS and refined to a resolution of 2.05 Å. The TgMIC2A/Ic core is organized into a central twisted beta sheet flanked by α-helices consistent with a canonical vWA fold. A restricted basic patch serves as the putative heparin binding site, but no heparin binding was detected in native gel shift assays. Furthermore, no metal was observed in the metal ion dependent adhesion site (MIDAS). Structural overlays with homologous A/I domains reveal a divergent organization of the MIDAS β4–α4 loop in TgMIC2A/Ic, which is stabilized through the burial of Phe195 into a deep pocket formed by Gly185. Intriguingly, Gly185 appears to be unique among A/I domains to TgMIC2A/I suggesting that the divergent loop conformation may also be unique to TgMIC2A/I. Although lacking the C-terminal extension, the TgMIC2A/Ic structure reported here is the first of an A/I domain from an apicomplexan parasite and provides valuable insight into defining the molecular recognition of host cells by these widespread pathogens.

Keywords: *Toxoplasma gondii*; microneme; MIC2; A/I domain; adhesion; X-ray crystallography

Additional Supporting Information may be found in the online version of this article.

Ognjen Grujic and Mark Pearce contributed equally to this work.

This work was supported by Canadian Institutes of Health Research (CIHR) grant MOP82915 to MJB. MLT is supported by a University of Victoria Graduate Fellowship. MJB is a CIHR New Investigator and a Michael Smith Foundation for Health Research (MSFHR) scholar.

**Correspondence to:* Martin J. Boulanger, Department of Biochemistry and Microbiology, University of Victoria, PO Box 3055 STN CSC, Victoria, BC V8W 3P6, Canada.
E-mail: mboulang@uvic.ca

Introduction

Apicomplexan parasites such as *Plasmodium* (malaria) and *Toxoplasma* (toxoplasmosis) are unique in their ability to bypass host cell uptake pathways, relying instead on parasite mediated active invasion. These obligate intracellular pathogens initiate the invasion process by secreting the contents of specialized apical complex organelles called micronemes.[1] One secreted protein of particular importance is micronemal protein 2 (TgMIC2) in *T. gondii* (thrombospondin-related anonymous protein (TRAP) in *Plasmodium* species),[2]

which is recognized as a critical virulence factor in promoting active invasion. Although attempts to completely knock-out TgMIC2 have been unsuccessful, conditional knock-outs resulted in reduced attachment and invasion capabilities by 78% and produced a nonlethal phenotype in mouse models of infection using up to 100 times the regular lethal dose.[3] The ability of MIC2 to play a central role in invasion is derived from its multimodular organization that effectively couples host cell recognition with the parasite's actin–myosin motor system.[4]

Full length TgMIC2 is a type 1 transmembrane protein comprised of a C-terminal cytoplasmic tail, a membrane spanning region, one degenerate and five conserved thrombospondin type 1 repeats (TSRs) forming a stalk like structure[5] capped by a single von Willebrand Factor A (vWA)–Integrin like A/I domain. In this organization, the A/I domain is optimally positioned to interact with host cell receptors.[6] In addition, TgMIC2 likely exists as a heterohexamer on the surface of *T. gondii* comprised of three MIC2 and three MIC2 associated protein (M2AP) molecules,[7] with M2AP associating with the TSRs (Harper and Carruthers, unpublished) [Fig. 1(A)]. There are currently no structures for any apicomplexan A/I domains despite their demonstrated importance in parasite adhesion and invasion and their proposed use as drug or vaccine targets.[8] Thus, elucidation of the TgMIC2A/I structure, albeit a truncated form, represents an important contribution toward guiding investigations into microneme protein-mediated invasion of host cells by apicomplexan parasites.

Results and Discussion

Design and production of TgMIC2A/I constructs

Sequence analysis of TgMIC2A/I confirmed strong homology with vWA and Integrin domains with a clearly defined N-terminal start site. However, defining the C-terminus was more complicated and prompted us to generate two constructs designated as TgMIC2A/Ic (conserved) and TgMIC2A/If (full). Both constructs begin at Thr72, downstream of the signal peptide and prosequence cleavage sites.[9] However, TgMIC2A/Ic terminates at Val220 [Fig. 1(B), green arrow], representing a core sequence conserved among the majority of vWA subfamilies,[6] and TgMIC2A/If terminates at Leu260 [Fig. 1(B), blue arrow], representing a general sequence homology within the vWA superfamily. Both constructs were produced in insect cells and purified to homogeneity. Unexpectedly, TgMIC2A/Ic eluted as dimer from the size exclusion column, whereas TgMIC2A/If eluted as a monomer, yet both migrated as expected on an SDS-PAGE gel [Fig. 1(C)]. The addition of tunicamycin increased the homogeneity of the purified proteins by inhibiting N-glycoslyation of Asn156 [Fig. 1(C)].

Overall structure

Crystallization trials were set with both TgMIC2A/I constructs, though diffraction quality crystals were only obtained for TgMIC2A/Ic. The structure was phased using iodide single isomorphous replacement and anomalous scattering (SIRAS) and refined to a resolution of 2.05 Å. Consistent with the size exclusion column profile [Fig. 1(C)], TgMIC2A/Ic crystallized as a dimer with a complexation significance score of 1.00 indicating the buried interface is energetically sufficient to promote assembly. Analysis of the TgMIC2A/Ic structure confirms the initial classification as a member of the TRAP family, and more broadly as a member of the vWA superfamily, with each monomer adopting a Rossmann fold of a central twisted beta sheet flanked with α-helices [Fig. 1(D), upper panel].[10] Interestingly, while most other A/I domains are organized primarily based on secondary structure elements, a single disulfide bond is present (Cys78–Cys164) in TgMIC2A/Ic that tethers the first beta strand to the third alpha helix [Fig. 1(D), lower panel].

Structural rationale for the observed TgMIC2A/Ic dimer

Although the TgMIC2A/Ic structure largely conforms to the canonical vWA fold, the surface exposed hydrophobic patch that promotes dimerization [Fig. 1(E), left panel] appears to result from the truncation of the C-terminus. Structural overlays reveal that a C-terminal region of two α-helices separated by a short β-strand in homologous vWA structures packs against the exposed hydrophobic patch in TgMIC2A/Ic [Fig. 1(E), right panel] effectively concealing it from solvent. Since the TgMIC2A/If construct adopts a monomer in solution, we conclude that the C-terminal extension serves a similar structural role in protecting a multimerization interface. Intriguingly, however, the C-terminal region in TgMIC2A/If differs significantly from related vWA domains [Fig. 1(B)] in that it displays a very high cysteine content (4/42 total residues) suggesting the formation of a highly stable "microdomain." This predicted structural divergence may also explain the ambiguity in defining the C-terminus. It is noteworthy that the C-terminus of TgMIC2A/If is only partially conserved with PfTRAP [Fig. 1(B), black box] further highlighting the novelty of this region. As we were unable to crystallize TgMIC2A/If, we attempted to solve the structure by small angle X-ray scattering (SAXS). Despite high quality data, we were unable to unambiguously orient the TgMIC2A/Ic structure within the molecular envelope calculated from the SAXS data and thus could not definitively establish the orientation of the C-terminal extension.

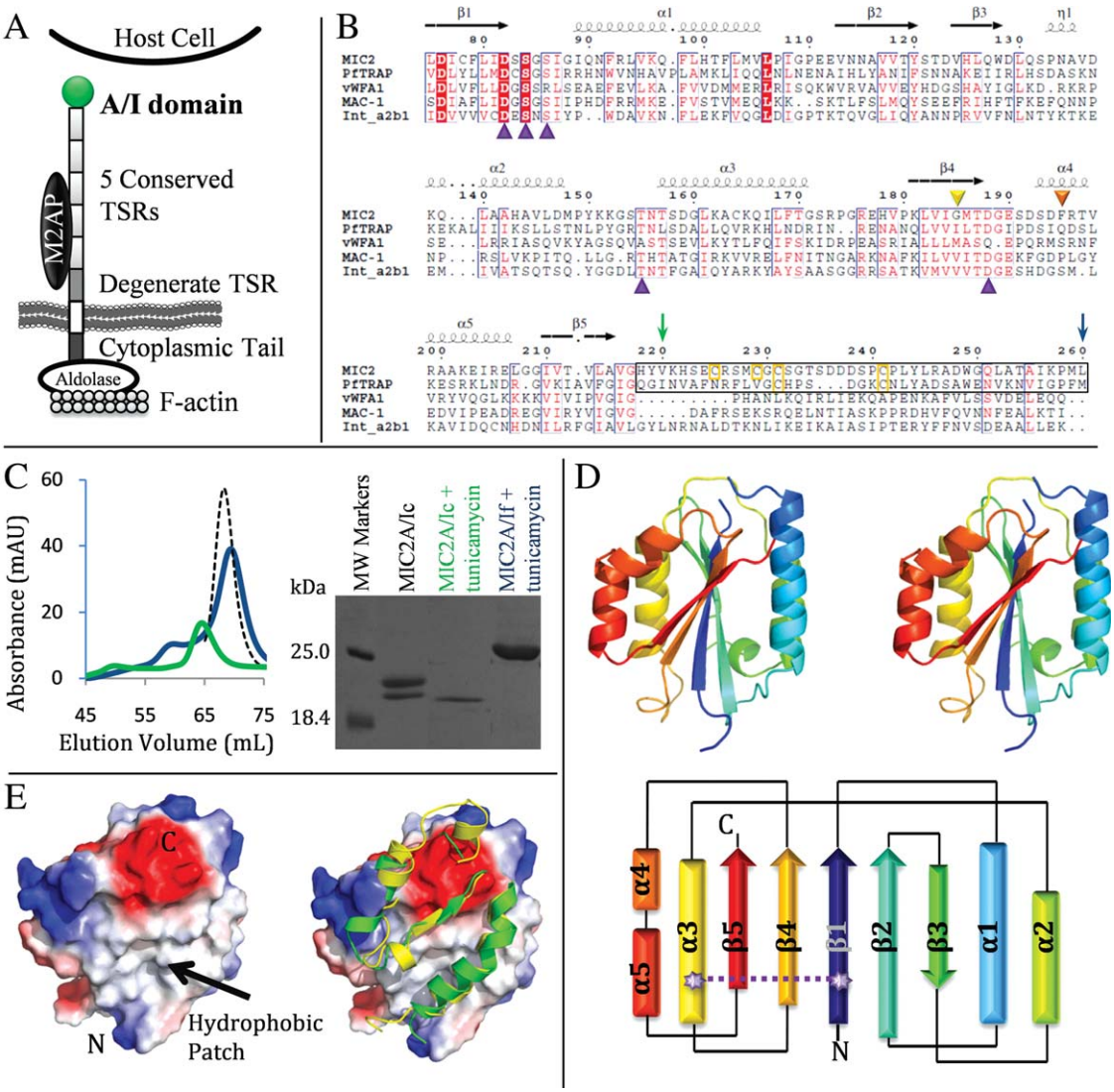

Figure 1. Biological assembly and overall structure of TgMIC2A/Ic. A: Single unit of the heterohexameric organization of TgMIC2, with the A/I domain (green sphere) positioned at the apical end of the full transmembrane protein. B: Sequence alignment of TgMIC2A/I with PfTRAP, vWFA1, Mac-1, and Integrin α2β1. MIDAS residues are indicated by purple triangles, C-terminal cysteines in orange boxes, divergent C-terminal region in black box and Gly185 and Phe195 as yellow and orange triangles, respectively. Secondary structure and residue numbering is indicated for TgMIC2A/I. C-terminii of TgMIC2A/Ic and TgMIC2A/If constructs demarcated by green and blue arrows, respectively. C: Size exclusion trace and associated SDS-PAGE gel of TgMIC2A/Ic (green) and TgMIC2A/If (blue) showing elution of TgMIC2A/Ic as dimer and TgMIC2A/Ic as a monomer with the carbonic anhydrase standard (29 kDa), shown as a dotted line. D: Stereo image of TgMIC2A/Ic colored from N (blue) to C (red) terminus, highlighting the conserved vWA fold and associated topology diagram with disulfide bond represented by a dotted line. E: Electrostatic surface of TgMIC2A/Ic reveals a hydrophobic patch at the dimer interface (left panel), which, in the structurally homologous integrin α2β1 (yellow, PDB ID 1AOX) and vWA (green, PDB ID 1AUQ), is concealed by the C-terminal extension (right panel).

A restricted basic surface patch likely requires multimerization for heparin binding

Harper *et al*. have demonstrated previously that TgMIC2A/I binds heparin independent of the metal ion dependent adhesion site (MIDAS)[11] implicating an additional contact surface. Despite having crystallized as a dimer, a clear basic patch comprising six basic residues from helices 3, 4, and 5 was observed on the TgMIC2A/Ic surface. Importantly, the analogous region in monomeric vWFA1 (PDB ID 1AUQ) is sufficient to coordinate heparin through an extensive network of four lysine residues[12] and an additional noncontiguous series of six residues[13] [Fig. 2(A)]. Overall, however, the basic patch on TgMIC2A/Ic is significantly smaller [Fig. 2(A)] than for vWFA1, though intriguingly similar in size to a proposed seven residue heparin binding surface on the homology model of PfTRAP.[14] Using native gel shift assays, we sought to determine whether either the monodisperse dimeric TgMIC2A/Ic or monomeric

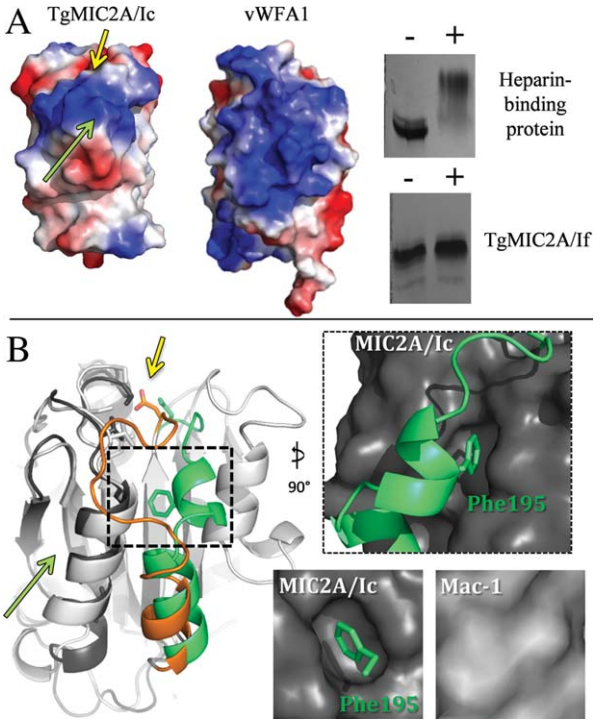

Figure 2. Structure–function analysis of TgMIC2A/I. (A) Left panel—electrostatic surface representation of TgMIC2A/Ic highlighting the spatially separated regions of potential functional importance: putative heparin-binding basic patch (green arrow) and the MIDAS (yellow arrow). Right panel—heparin binding native gel shift assay in the presence (+) and absence (–) of heparin for a known heparin binding protein and TgMIC2A/If. No heparin binding was observed with TgMIC2AI/f. (B) Left panel—Overlay of TgMIC2A/Ic (dark gray) and Mac-1 (light grey, PDB ID 1BHO) highlighting the reorganized alpha 4 and 5 helices in TgMIC2A/Ic (green) compared to the analogous regions in Mac-1 (orange). TgMIC2A/Ic Phe195 on α4, anchors the α4 helix by docking into a deep pocket made possible by Gly185. Ultimately, this reorganized loop results in Asp188 of the MIDAS motif being shifted 4.4 Å from the analogous Asp of Mac-1 effectively eliminating the ability to coordinate a metal.

TgMIC2A/If was able to bind heparin. Despite a clear band shift observed with the positive control, no heparin binding was detected with either TgMIC2A/Ic or TgMIC2A/If where the latter construct is potentially more biologically relevant as additional residues at the C-terminus may augment the basic patch observed in TgMIC2A/Ic [Fig. 2(A)]. These results are consistent with previous findings by Harper *et al*. where the authors showed that a large, multimeric species of TgMIC2A/I was necessary to bind heparin.[11]

A reorganized TgMIC2A/Ic does not appear to present a functional MIDAS motif

A generally conserved characteristic of the vWA superfamily is the presence of a cation binding (typically Mg^{2+} or Mn^{2+}) MIDAS motif comprised of a DxSxS sequence with an additional Asp and Thr distal in primary sequence [Fig. 1(B), purple triangles], but spatially proximal in the tertiary structure. Point mutation studies on the Thr and Asp residues outside of the DxSxS motif of PfTRAP showed decreased sporozoite infectivity,[15] but no metal-dependent interaction has been defined thus far. Although TgMIC2A/I harbors a fully conserved MIDAS motif (Asp82, Ser84, Ser86, Thr155, and Asp188), extensive soaking with high concentrations (20 m*M*) of Mg^{2+} or Mn^{2+} did not yield a bound metal. Overlays with a variety of vWA and Integrin domains revealed that Asp188, located on the β4–α4 loop of TgMIC2A/Ic, is shifted nearly 4 Å away from the expected metal coordination site [Fig. 2(B)]. This shift results from the displacement of helix α4, which is positioned within 9 Å of the hydrophobic patch. Although we are mindful that the position of helix α4 may be an artifact derived from the truncation of the C-terminus in TgMIC2A/Ic, structural analysis suggests an intriguing alternative. The divergent loop structure in TgMIC2A/Ic is anchored by a highly stabilizing knob and hole type interaction between Phe195 [Fig. 1(B), orange triangle] on helix α4 and a deep pocket formed by Gly185 [Fig. 1(B), yellow triangle] on strand β4 [Fig. 2(B), upper right panel]. By comparison, the analogous residue to TgMIC2A/I Gly185 in Mac-1 is a Val, effectively eliminating the possibility of any significant pocket [Fig. 2(B), lower right panels]. In fact, despite aligning more than 20 sequences (Supporting Information Fig. S1), we have yet to identify another A/I domain with an analogous glycine at position 185 suggesting that TgMIC2A/I may be uniquely capable of stabilizing the observed conformation. It is possible that the TRAP A/I domain from the closely related *Neospora caninum* adopts a similar conformation, though, replacement of Gly185 at the bottom of the hydrophobic pocket with an alanine in *N. caninum* will likely prevent complete burial of the conserved Phe resulting in a weaker interaction. It is interesting to note that the C-terminal region of both TgMIC2A/I and NcTRAP includes four cysteines consistent with a similar architecture, while the homologous protein from the more distantly related coccidian *Eimeria* does not encode the conserved Gly/Ala, Phe, or four C-terminal cysteines indicating a significantly divergent structure.

Materials and Methods

Bioinformatics

Multiple sequences were aligned using ClustalW[16] and illustrated in ESPript.[17] Accession numbers for aligned sequences are as follows; *T. gondii* MIC2A/I (XP_002367474.1), *P. falciparum* TRAP (AAC18657.1), human von Willebrand Factor A (157830097), human

integrin Mac-1 (157838286), and human Integrin α2β1 (4139906).

Cloning, protein expression, and purification

Constructs encoding the conserved (residues 72–220) and full (residues 72–260) forms of the TgMIC2A/I domain were generated from *T. gondii* type II genomic DNA and cloned into a modified pAcGP67B vector (Pharmingen). Each clone was transfected with linearized Baculovirus DNA into Sf-9 insect cells and the resultant viruses amplified to high titre. For each construct, 3 L of Hi-5 cells at 1.8×10^6 cells/mL were infected with amplified virus, and tunicamycin was added to a final concentration of 0.3 μg/mL. After 65 h, the supernatants were harvested, concentrated, and the TgMIC2A/I proteins purified using nickel affinity and size exclusion chromatography. Fractions were analyzed by SDS-PAGE, pooled based on purity, and the hexahistidine tag removed by digestion with thrombin. Final yield for each recombinant protein was ~0.2 mg/L of culture.

Crystallization, data collection, and processing

Crystallization trials with TgMIC2A/Ic were set using Index and PEG/Ion screens (Hampton Research) in 96 well sitting drop plates (Emerald Biosystems). The final drops consisted of 1 μL TgMIC2A/Ic at 12 mg/mL buffered in HBS (20 m*M* HEPES pH 8, 150 m*M* NaCl) plus 1 μL reservoir solution equilibrated against 100 μL reservoir solution. Crystals grew overnight in 27% PEG 3350, 0.1*M* HEPES pH 7.5, 0.2*M* ammonium sulfate. A single crystal was cryo protected in mother liquor plus 15% glycerol and 15% ethylene glycol for 30 s and flash cooled at 100 K directly in the cryo stream. For the iodide derivative, the cryo mixture was supplemented with sodium iodide to a final concentration of 1*M* and the soak was extended to 60 s. Diffraction data were collected on a Rigaku R-axis IV++ area detector coupled to an MM-002 X-ray generator with Osmic "blue" optics and an Oxford Cryostream 700. Native TgMIC2A/I crystals diffracted to 2.05 Å and the TgMIC2A/I iodide derivative to 2.75 Å using a 180-s exposure and 0.5° oscillation. Diffraction data were processed using Crystal Clear software with d*trek.[18]

Phasing and model refinement

A total of 15 iodide sites were identified and refined using autoSHARP.[19] High quality phases were obtained using SIRAS. Automated building with ARP/Warp[20] was used to register and build ~70% of the sequence. The remaining structure was built manually and solvent atoms selected using COOT[21] and refined with REFMAC[22] to an R_{cryst} of 21.0 and an R_{free} of 27.8%. Electron density surrounding the apical tip of the β1–α1 loop in chain B and the end of the β4–α4 loop in chain A was poorly defined, and thus, these regions were largely modeled based on overlays with the alternate chain. All solvent atoms were inspected manually before deposition. Stereochemical analysis was performed using PROCHECK and SFCHECK in CCP4.[23] Overall 5% of the reflections were set aside for calculation of R_{free}. Data collection and refinement statistics are presented in Table I. The coordinates and structure factors have been deposited into the Protein Data Bank under accession codes 2XGG and r2XGGsf, respectively.

Table I. *Data Collection and Refinement Statistics*

A: Data collection	
Space group	$P4_{1/3}2_12$
a, *b*, *c* (Å)	63.03, 63.03, 157.63
Measured reflections	221,820
Unique reflections	20,754
Redundancy	10.69 (10.82)
Completeness (%)	100.0 (100.0)
$I/\sigma(I)$	15.9 (4.7)
R_{merge}[a]	0.057 (0.433)
B: Refinement statistics	
Space group	$P4_32_12$
Resolution range (Å)	24.84–2.05 (2.10–2.05)
R_{cryst}[b]/R_{free}[c]	0.210/0.278 (0.252/0.361)
No. of atoms	
Protein	2252
Solvent	104
Glycerol	6
B-values	
Protein (Å^2)	43.43
Solvent (Å^2)	51.65
Glycerol (Å^2)	66.78
r.m.s. deviation from ideality	
Bond lengths (Å)	0.023
Bond angles (°)	2.002
Ramachandran plot (%)	
Favourable	87.1
Allowed	11.7
Generously allowed	1.2
Disallowed	0

Values in parentheses are for the highest resolution shell.
[a] $R_{merge} = \sum_{hkl}\sum_i |I_{hkl,i} - [I_{hkl}]| / \sum_{hkl}\sum_i I_{hkl,i}$, where $[I_{hkl}]$ is the average of symmetry related observations of a unique reflection.
[b] $R_{cryst} = \sum |F_{obs} - F_{calc}| / \sum F_{fobs}$, where F_{obs} and F_{calc} are the observed and the calculated structure factors, respectively.
[c] R_{free} is R using 5% of reflections randomly chosen and omitted from refinement.

Native gel shift assays

Purified protein in HBS buffer was incubated for 30 min at room temperature with heparin sodium salt (Sigma) in a 1:5 protein to heparin molar ratio. Reactions with TgMIC2A/Ic and TgMIC2A/If were carried out in the presence and absence of 10 m*M* $MgCl_2$, and solutions were run on 8–25% gradient gels using native buffer strips and the PhastGel system (GE Healthcare).

Conclusions

The 2.05 Å resolution structure of TgMIC2A/Ic represents the first structural characterization of an A/I domain from an apicomplexan parasite. Despite what

turned out to be a truncation of the ambiguously defined C-terminus, our structure offers unique insight into both the previously defined requirement for TgMIC2A/I multimerization in order to bind heparin and the metal binding capabilities of the MIDAS motif. Collectively, this study represents an important step forward in establishing a structural basis for MIC2 dependant sensing of the host cell by *T. gondii*.

References

1. Carruthers VB, Giddings OK, Sibley LD (1999) Secretion of micronemal proteins is associated with toxoplasma invasion of host cells. Cell Microbiol 1:225–235.
2. Templeton TJ, Kaslow DC (1997) Cloning and cross-species comparison of the thrombospondin-related anonymous protein (TRAP) gene from *Plasmodium knowlesi*, *Plasmodium vivax* and *Plasmodium gallinaceum*. Mol Biochem Parasitol 84:13–24.
3. Huynh MH, Carruthers VB (2006) Toxoplasma MIC2 is a major determinant of invasion and virulence. PLoS Pathog 2:e84.
4. Jewett TJ, Sibley LD (2003) Aldolase forms a bridge between cell surface adhesins and the actin cytoskeleton in apicomplexan parasites. Mol Cell 11:885–894.
5. Tan K, Duquette M, Liu JH, Dong Y, Zhang R, Joachimiak A, Lawler J, Wang JH (2002) Crystal structure of the TSP-1 type 1 repeats: a novel layered fold and its biological implication. J Cell Biol 159:373–382.
6. Wan KL, Carruthers VB, Sibley LD, Ajioka JW (1997) Molecular characterisation of an expressed sequence tag locus of *Toxoplasma gondii* encoding the micronemal protein MIC2. Mol Biochem Parasitol 84:203–214.
7. Jewett TJ, Sibley LD (2004) The toxoplasma proteins MIC2 and M2AP form a hexameric complex necessary for intracellular survival. J Biol Chem 279:9362–9369.
8. Morahan BJ, Wang L, Coppel RL (2009) No TRAP, no invasion. Trends Parasitol 25:77–84.
9. Carruthers VB, Sherman GD, Sibley LD (2000) The Toxoplasma adhesive protein MIC2 is proteolytically processed at multiple sites by two parasite-derived proteases. J Biol Chem 275:14346–14353.
10. Whittaker CA, Hynes RO (2002) Distribution and evolution of von Willebrand/integrin A domains: widely dispersed domains with roles in cell adhesion and elsewhere. Mol Biol Cell 13:3369–3387.
11. Harper JM, Hoff EF, Carruthers VB (2004) Multimerization of the *Toxoplasma gondii* MIC2 integrin-like A-domain is required for binding to heparin and human cells. Mol Biochem Parasitol 134:201–212.
12. Emsley J, Cruz M, Handin R, Liddington R (1998) Crystal structure of the von Willebrand Factor A1 domain and implications for the binding of platelet glycoprotein Ib. J Biol Chem 273:10396–10401.
13. Rastegar-Lari G, Villoutreix BO, Ribba AS, Legendre P, Meyer D, Baruch D (2002) Two clusters of charged residues located in the electropositive face of the von Willebrand factor A1 domain are essential for heparin binding. Biochemistry 41:6668–6678.
14. Akhouri RR, Bhattacharyya A, Pattnaik P, Malhotra P, Sharma A (2004) Structural and functional dissection of the adhesive domains of *Plasmodium falciparum* thrombospondin-related anonymous protein (TRAP). Biochem J 379:815–822.
15. Matuschewski K, Nunes AC, Nussenzweig V, Menard R (2002) Plasmodium sporozoite invasion into insect and mammalian cells is directed by the same dual binding system. EMBO J 21:1597–1606.
16. Thompson JD, Higgins DG, Gibson TJ (1994) CLUSTAL W: improving the sensitivity of progressive multiple sequence alignment through sequence weighting, position-specific gap penalties and weight matrix choice. Nucleic Acids Res 22:4673–4680.
17. Gouet P, Courcelle E, Stuart DI, Metoz F (1999) ESPript: multiple sequence alignments in PostScript. Bioinformatics 15:305–308.
18. Pflugrath J (1999) The finer things in X-ray diffraction data collection. Acta Crystallogr Sect D 55: 1718–1725.
19. Vonrhein C, Blanc E, Roversi P, Bricogne G (2007) Automated structure solution with autoSHARP. Methods Mol Biol 364:215–230.
20. Perrakis A, Morris R, Lamzin VS (1999) Automated protein model building combined with iterative structure refinement. Nat Struct Biol 6:458–463.
21. Emsley P, Cowtan K (2004) Coot: model-building tools for molecular graphics. Acta Crystallogr Sect D 60: 2126–2132.
22. Murshudov GN, Vagin AA, Dodson EJ (1997) Refinement of macromolecular structures by the maximum-likelihood method. Acta Crystallogr Sect D 53:240–255.
23. Collaborative Computational Project Number 4 (1994) The CCP4 Suite—programs for protein crystallography. Acta Crystallogr Sect D 50:760–763.